Performance evaluation of natural iron-rich sandy soil as a low-cost adsorbent for removal of lead from water

Yee Sern Ng[a], Bhaskar Sen Gupta[b,1], Mohd Ali Hashim[a,*]

[a]*Faculty of Engineering, Department of Chemical Engineering, University of Malaya, 50603 Kuala Lumpur, Malaysia,*
email: yeesern86@yahoo.com (Y.S. Ng), Tel. +60 3 79675296; Fax: +60 3 79675319;
email: alihashim@um.edu.my (M.A. Hashim)
[b]*School of the Built Environment, Heriot-Watt University, Edinburgh Campus, EH14 4AS Edinburgh, Scotland, UK,*
Tel. +44(0)131 451 8171; email: b.sengupta.hw.ac.uk (B.S. Gupta)

ABSTRACT

Technical feasibility of natural iron-rich sandy soil as a low-cost adsorbent for removal of lead from water was investigated . The soil, which had an iron content of 3,719 mg/kg, was collected from Hulu Langat, Malaysia, and was used for adsorption studies without any surface modification through chemical treatment. The effects of pH, solution: soil ratio and initial lead concentration on the adsorption efficiency were studied using response surface methodology based on Box–Behnken experimental design. The results showed that pH of the solution had the highest impact on the adsorption efficiency whereby adsorption efficiency of 97% could be achieved at pH 3.5–5. The experimental data were also checked for compliance with different kinetic models and adsorption isotherms. The adsorption process was found to be rapid monolayer chemisorption with adsorption capacity of 0.9–1.0 mg/g, as it fitted Langmuir isotherm and followed pseudo-second-order kinetic model.

Keywords: Natural iron-rich sandy soil; Lead; Adsorption; Adsorption kinetics; Adsorption isotherm

1. Introduction

Lead is reported as a highly toxic material whereby the maximum allowable concentration in water is 0.1 ppm for standard A (effluent that is discharged upstream of a water supply intake) and 0.5 ppm for standard B (effluent that is discharged downstream of a water supply intake) in Malaysia [1]. Lead often contaminates water bodies as well as soil environment via different sources such as fertilisers, pesticides, metal mining, milling and smelting processes [2,3]. Inhalation and ingestion of lead can cause poisoning and even death to human as it accumulates in the organs. Lead can cause serious health effects such as loss of memory/brain damage, nausea, insomnia, anorexia and weakness of joints. Moreover, it may also inhibit the synthesis of haemoglobin, causing dysfunction on kidneys, joints and systems such as reproductive system, cardiovascular system, central

*Corresponding author.

[1]Former affiliation: School of Planning, Architecture and Civil Engineering, Queen's University Belfast, David Keir Building, Belfast BT9 5AG, UK

nervous system and peripheral nervous system [2,3]. Therefore, it is necessary to ensure that lead is effectively removed from water before consumption.

Adsorption is one of the water treatment techniques for removing heavy metals. It is the most favourable method due to its simple design [4] and it does not add undesirable by-products [5]. Several types of adsorbents have been studied by researchers on lead removal from water such as activated carbons [6–10], resin [11], treated acorn waste [12], sea nodule [13], copolymer [14], pomegranate peel [15] and clays [16–19]. Metal oxides such as iron oxides, manganese oxides and aluminium oxides were also used for lead adsorption, taking advantage of their high surface area and charge for trapping metal ions [20–24]. Iron oxides are often coated on supports such as sand and crushed brick [20–23], and lead adsorption capacities of 0.34–5.49 mg/g are reported for these coated sands [20–23].

In this study, natural high-iron sandy soil from Hulu Langat, Malaysia, was used as a low-cost adsorbent for adsorption of dissolved lead in water without further surface modification through chemical treatment. The feasibility of the adsorbent was evaluated by investigating the effects of pH, solution: soil ratio and initial lead concentration on lead adsorption. The study was conducted using response surface methodology (RSM) based on Box–Behnken experimental design in order to assess the interaction effects between the key operating parameters. Moreover, the adsorption isotherm and kinetics for lead on the soil were also evaluated using various models to establish the adsorption mechanism as well as adsorption capacity of the soil.

2. Materials and methods

2.1. Chemicals and materials

Lead nitrate, $Pb(NO_3)_2$, nitric acid and sodium hydroxide were supplied by R&M Chemicals, Malaysia. The adsorbent used in this study was natural sandy soil with high-iron content (maghemite), obtained from Hulu Langat, Malaysia. The soil was naturally dried to remove moisture and was sieved to <0.85 mm size before use. The characteristics of the soil are shown in Table 1.

2.2. Response surface methodology

Technical feasibility of the natural iron-rich soil as low-cost adsorbent under different operating parameters was evaluated using RSM as this technique requires fewer experiments than normal factorial design. RSM is a collection of mathematical and statistical techniques that are useful for the modelling and analysis of problems for which a response on outcome is influenced by several variables [25]. An approximation for the true functional relationship between the independent variables and the response can be obtained by RSM and analysis of variance (ANOVA) in the form of polynomial equation, as shown in (Eq. (1)) where y is the response, β is the regression coefficient, and x are the independent parameters [25].

$$y = \beta_0 + \sum_{i=1}^{3} \beta_i x_i + \sum_{i=1}^{3} \beta_{ii} x_i^2 + \sum_{i=1}^{2} \sum_{j=i+1}^{3} \beta_{ij} x_i x_j \quad (1)$$

In this study, Box–Behnken experimental design was used. This is a spherical three level design by combining 2^k factorial with incomplete block design, and it is generally efficient in terms of number of required runs in comparison with central composite design [25]. Three parameters were investigated in the present work, namely: (i) pH of the solution, (ii) solution: soil ratio and (iii) initial lead concentration, which have a bearing on its speciation in the solution as well as the effective contact area between lead and the soil surface, thus affecting the adsorption performance. The levels for each parameter are as shown in Table 2. Table 3 shows that a total number of 17 experiments are suggested by Box–Behnken design, with five replicates centre point experiment (Level = 0) for estimating the errors. The experiments were conducted in random sequences as suggested by the design to minimise the unknown nuisance effect on the response, which was the adsorption efficiency in this study.

2.3. Adsorption test

Adsorption test was conducted by mixing 10 g of soil with $Pb(NO_3)_2$ solution at different operating parameters in a conical flask. The mixture was then homogenised using a mechanical shaker at 150 rpm for 24 h at room temperature. Liquid sample was taken after the experiment, and suspended particles were removed by filtration. Lead concentration in the aqueous sample was determined by ICP-OES, and the adsorption efficiency was calculated using (Eq. (2)). The sequence of the experiments and the results are as shown in Table 3.

$$\text{Adsorption efficiency}, \% = \frac{\text{Initial Pb concentration} - \text{Final Pb concentration}}{\text{Initial Pb concentration}}$$

$$(2)$$

Table 1
Characteristic of natural iron-rich sandy soil

Soil particle size distribution		Soil metal content	
Sand (>50 μm)	92%	Iron (mg/kg)	3,719
Silt (2–50 μm)	6%	Aluminium (mg/kg)	2,400
Clay (<2 μm)	2%	Manganese (mg/kg)	185
Soil properties	Value	Magnesium (mg/kg)	635
pH	3.97	Lead (mg/kg)	11
Specific gravity	2.5	Zinc (mg/kg)	18
CEC (meq/100 g)	5.1		
Organic matter content	1.4%		

Table 2
The level and range of the parameters studied

Symbol	Parameters	Level		
		−1	0	1
A	pH	2	3.5	5
B	Solution:soil ratio (mL/g)	1	5.5	10
C	Initial lead concentration (ppm)	20	60	100

2.4. Adsorption capacity and kinetic study

The capacity of sandy soil for lead adsorption was determined from shake flask study by contacting 10 g of soil with 200 mL of 150 ppm lead solution. The mixture was vigorously shaken in an orbital shaker at 175 rpm. Lead concentration in the solution at different time interval was analysed using ICP-OES, and the adsorption capacity of the soil was calculated using (Eq. (3)). The adsorption data were fitted to six kinetic models, namely pseudo-first-order kinetic model, pseudo-second-order kinetic model, Elovich model, second-order kinetic model, film diffusion mass transfer kinetic model and double exponential model.

calculated using (Eq. (3)). The data obtained for equilibrium lead concentration in both solution and soil were fitted to four isotherm models, namely Langmuir isotherm, Freundlich isotherm, Temkin isotherm and Dubinin–Radushkevich isotherm.

3. Results and discussion

3.1. Characterisation and surface morphology of sandy soil

Characterisation study was carried out for the virgin soil. The results for FTIR as shown in Fig. 1(a) suggest that the soil is mainly silicon dioxide with high silicon (Si) content as most of the peaks observed are Si related such as Si–O–Si stretching (peak: 1,035.7–1,084.02 cm^{-1}), Si–C stretching (peak: 2,359.02 cm^{-1}) and O–H stretching (peak: 3,447.53–3,694.62 cm^{-1}) [26]. In addition, the Fe–O stretch peaks at 464.64, 529.23, 690.32 and 781.95 cm^{-1} also indicated the presence of maghemite as the main iron species in this soil [27–29]. BET analysis shows that the sandy soil has surface area of 2.3126 m^2/g, with limited pore volume and average pore size of 0.0012 cm^3/g and 20.4 nm, respectively. Fig. 1(b) depicts that the nitrogen adsorption–desorption isotherm on the sandy soil at 77 K is an

$$\text{Adsorption capacity, mg/kg} = \frac{\text{Initial Pb in the solution} - \text{Final Pb inthe solution, mg}}{\text{Mass of soil used, kg}} \qquad (3)$$

2.5. Adsorption isotherm

Each batch of adsorption test was carried out with 4 g of soil and 100 mL lead solution having lead concentration, ranging from 20 ppm to 100 ppm. The tests were conducted for five hours in an orbital shaker at a rotational speed of 175 rpm. The lead concentration in the solution before and after adsorption was determined by ICP-OES, and the adsorption by soil was

intermediate between type II and type IV isotherm with a hysteresis loop, as per IUPAC guideline [30,31]. This trend suggested that the soil was generally a non-porous/macroporous material, with limited mesopores for capillary condensation [30,31]. The mesopores could be mainly due to the rough surface on the soil, as depicted in Fig. 1(c) from the result of scanning electron microscope (SEM). The rough surface could be attributed to the deposition of iron and other minerals

Table 3
Parameters studied in Box–Behnken design and the experimental results

Std	Run	Block	pH	Solution:soil ratio	Initial concentration (ppm)	Final concentration (ppm)	Adsorption efficiency (%)
9	1	Block 1	3.5	1	20	2.72	86.41
5	2	Block 1	2	5.5	20	17.83	10.84
6	3	Block 1	5	5.5	20	1.57	92.15
14	4	Block 1	3.5	5.5	60	12.12	79.79
7	5	Block 1	2	5.5	100	80.85	19.15
15	6	Block 1	3.5	5.5	60	12.95	78.42
12	7	Block 1	3.5	10	100	2.56	97.44
16	8	Block 1	3.5	5.5	60	9.74	83.76
4	9	Block 1	5	10	60	23.60	60.67
13	10	Block 1	3.5	5.5	60	12.89	78.51
11	11	Block 1	3.5	1	100	2.72	97.28
17	12	Block 1	3.5	5.5	60	10.96	81.73
1	13	Block 1	2	1	60	54.42	9.3
3	14	Block 1	2	10	60	58.38	2.71
10	15	Block 1	3.5	10	20	1.65	91.77
8	16	Block 1	5	5.5	100	18.08	81.92
2	17	Block 1	5	1	60	3.04	94.94

on the soil, which was in line with the observations made by Boujelben et al. [21] and Ahmedzeki [20]. However, it is observed from Fig. 1(d) that significant pore reduction occurred after the adsorption experiment, suggesting the interaction between lead solution and soil interface, as well as lead adsorption on the soil surface.

3.2. ANOVA analysis and model diagnosis

ANOVA is an important tool in statistical analysis. It analyses the impact of experimental parameters in affecting the response. Table 4 shows ANOVA for the adsorption efficiency. There are three parameters, namely pH (A), solution: soil ratio (B) and initial concentration (C). The model has F-value of 2,029.57 with probability $> F$ of less than 0.0001. This indicates that the model has significant confidence level of >99% as there is only 0.01% chance that the model F-value this large could occur due to noise. Besides that, the "lack of fit F-value" of 3.15 also implies that the lack of fit for the proposed mathematical model relative to pure error is not significant. There is 14.84% chance that the lack-of-fit F-value this large could occur due to noise. Non-significant lack of fit is good and the model fits well with the experimental data. From the model, it is found that pH (Parameter A) has more dominant effect than solution: soil ratio and initial concentration of the system as it has lowest Probability $> F$ value at <0.0001 in comparison with solution: soil ratio (0.4127) and initial lead concentration (0.1469). Other parameters A^2, C^2, AB, AC and A^2B which have

Probability $> F$ of less than 0.05 are considered as significant model terms.

In terms of goodness-of-fit R^2, the difference between predicted R^2 (0.9687) and adjusted R^2 (0.9912) confirms that the model fits the experimental data well. Moreover, an adequate precision of >4 (38.5851) for this model further justifies the adequacy of the model. The model's validity is further strengthened by the diagnosis of normal probability plot, as shown in Fig. 2(a), whereby no abnormality is found in the model. Also, Fig. 2(b) shows that the predicted value fits the actual result well as they have a deviation of 3.17% only (less than 5%). Thus, the mathematical model proposed is statistically valid for space naviga-tion, as shown in (Eq. (4)), where A, B and C repre-sent the pH (2–5), solution: soil ratio (1–10) and initial concentration (20–100 ppm), respectively.

$$\begin{aligned} \text{Adsorption efficiency}, \% = {} & -159.13129 + 115.76367A \\ & - 11.13131B - 0.50492C \\ & - 11.64526A^2 + 0.090691B^2 \\ & + 6.84156 \times 10^{-3}C^2 \\ & + 6.99111AB - 0.077250AC \\ & - 1.14519A^2B \end{aligned}$$

$$(4)$$

3.3. Effect of pH and solution: soil ratio on adsorption efficiency

Fig. 3 shows the effect of solution: soil ratio as well as pH on the efficiency of lead adsorption on the
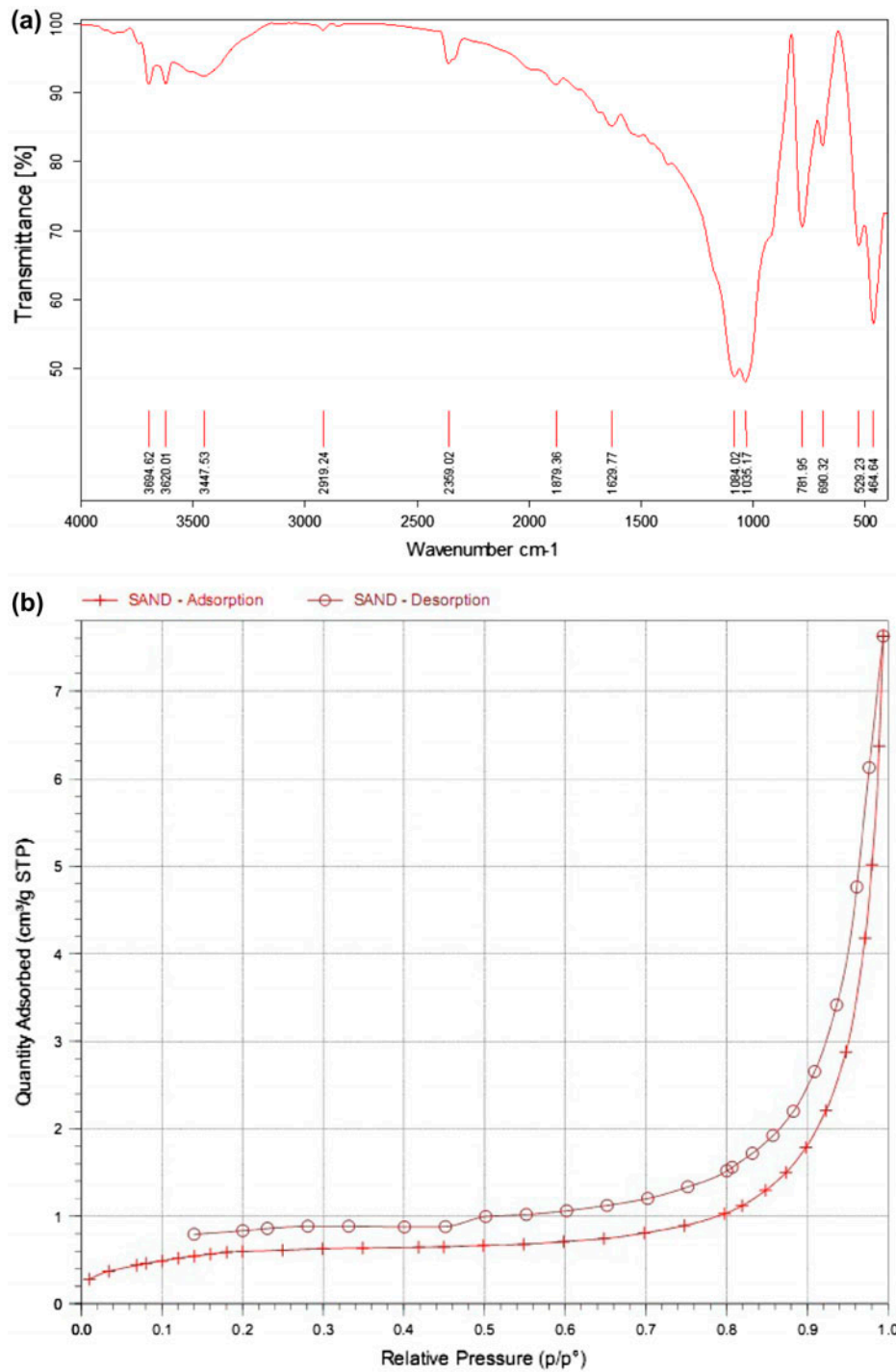
Fig. 1. Characterisation study for the sandy soil: (a) FTIR spectra, (b) adsorption–desorption isotherm for nitrogen at 77 K, (c) SEM analysis on surface morphology of the virgin soil, and (d) SEM analysis on surface morphology of the soil after adsorption.

sandy soil. The pH range in this study was 2–5 as lead hydroxide precipitation was observed at pH 6 and above. The result revealed that the pH of the aqueous solution strongly influenced the adsorption process, whereby higher pH showed better adsorption efficiency. This is in line with the works of other researchers which claimed that higher adsorption was achieved at higher pH in the range of 2–6 [20–24].
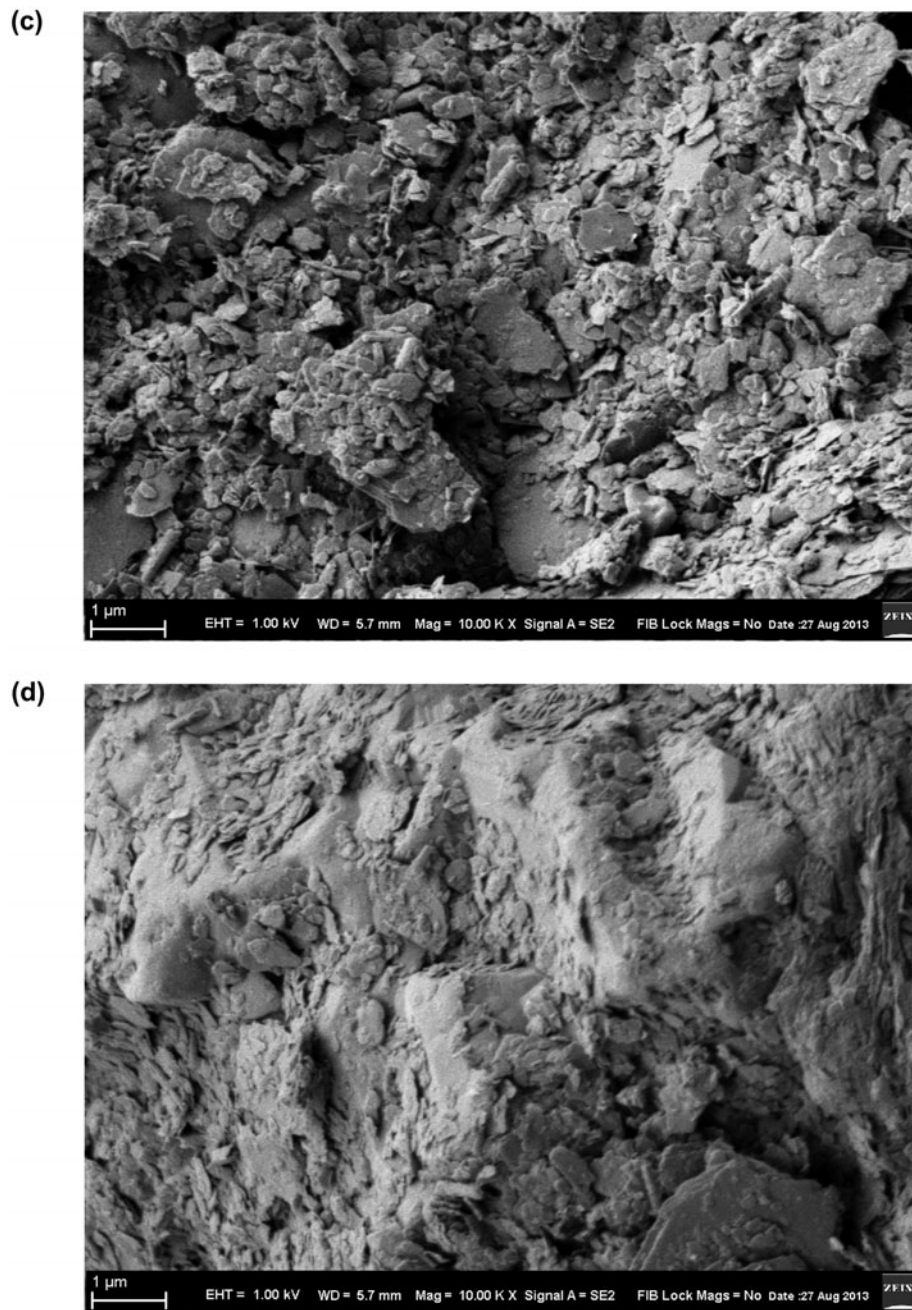
Fig. 1. (*Continued*).

Adsorption competition between lead and proton could occur at low pH condition [17,24]. Besides that, the adsorption of protons on soil surface which impart a positive charge to the soil may induce electrostatic repulsion between soil and lead ions as well [17,32,33]. Moreover, possible dissolution of iron from soil could be another reason for low Pb adsorption as the number of binding site had been reduced under low pH condition. These phenomena could be the main reason for low adsorption efficiency at low pH. In contrast, higher pH increased the number of negatively charged sites on soil surface via surface deprotonation and this enhanced the electrostatic attraction between lead ions and soil surface, which increased the adsorption efficiency [23,32,33].

The pH was also found to influence the effect given by solution: soil ratio. Under low pH condition, the increase in solution: soil ratio only affects the

Table 4
ANOVA analysis for adsorption efficiency

| Source	Sum of squares	DF	Mean square	F value	Prob. > F	
Model	18,266.16	9	202.9	202.09	<0.0001	Significant
A	10,344.97	1	10,344.97	1,030.09	<0.0001	
B	7.62	1	7.62	0.76	0.4127	
C	26.72	1	26.72	2.66	0.1469	
A^2	6,863.24	1	6,863.24	683.40	<0.0001	
B^2	14.20	1	14.20	1.41	0.2732	
C^2	504.53	1	504.53	50.24	0.0002	
AB	191.55	1	191.55	19.07	0.0033	
AC	85.93	1	85.93	8.56	0.0222	
A^2B	268.89	1	268.89	26.77	0.0013	
Residual	70.30	7	10.04			
Lack of fit	49.39	3	16.46	3.15	0.1484	Not significant
Pure error	20.91	4	5.23			
Cor total	18,336.46	16				
Std. Dev.	3.17		R^2	0.9962		
Mean	67.46		Adjusted R^2	0.9912		
CV	4.70		Predicted R^2	0.9687		
Press	574.13		Adequate precision	38.5851		
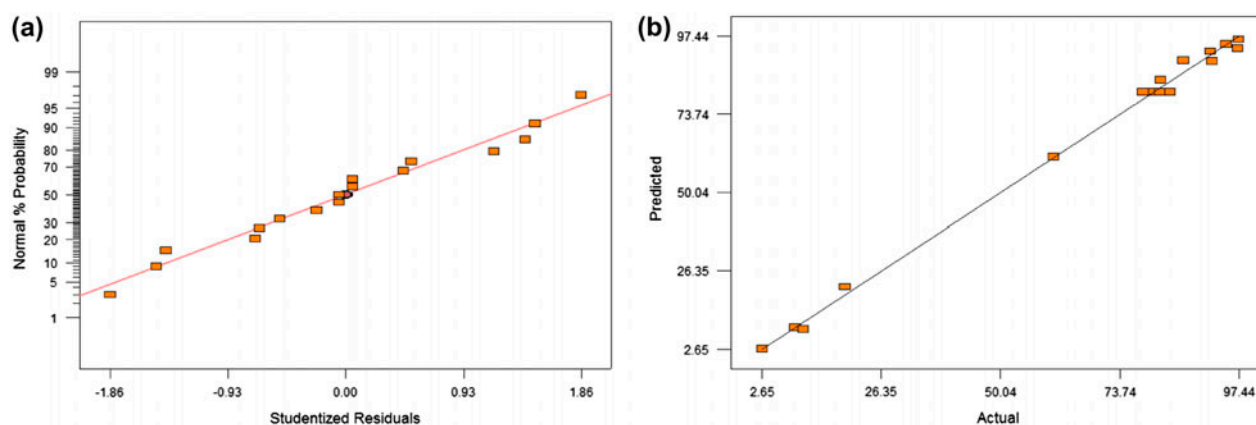
Fig. 2. (a) Normal probability plot for the data and (b) Predicted results and actual results for adsorption efficiency.

removal efficiency slightly, as illustrated in Fig. 3. At pH 2, the increase in solution: soil ratio from 1 to 10 only reduces the adsorption efficiency from 9.3 to 2.71%. However, at pH of 5, the adsorption efficiency was found to reduce greatly from 94.94 to 60.67%. Reduction in adsorption efficiency was expected when the solution: soil ratio was increased, lowering the specific contact area for effective collision between the soil and solution, as reported by Chaari et al. and Ahmedzeki [17,20]. Under low pH condition, lower availability of binding sites limited lead adsorption onto soil compared to the decrement in the specific contact area between the soil and solution when

solution: soil ratio was increased. In contrast, high pH condition provided higher number of binding sites and thus the effect of decrease in specific contact area became much more significant when solution: soil ratio was increased.

3.4. Effect of pH and initial lead concentration on adsorption efficiency

Fig. 4 shows that initial lead concentration has minor effect on adsorption efficiency, and the effect is strongly dependent on the pH of the system. The use of higher initial concentration from 20 to 100 ppm at

pH 2 increased the adsorption efficiency from 10.84 to 19.15%. At this pH, lead adsorption was low as there was limited number of binding sites available. As the initial concentration increased, higher collision rate between lead and soil surface occurred [34], which offered a higher chance of lead adsorption via binding on the soil. Consequently, the adsorption efficiency was enhanced. However, a different observation was made as the pH was increased to 5. Adsorption efficiency slightly decreased from 92.15 to 81.92% when the initial concentration was increased from 20 to 100 ppm. This trend was also observed in the work of Chaari et al. [17] and Ahmedzeki [20]. However, it was worth noting that this was mainly due to mathematical calculation of the adsorption efficiency. Chaari et al. [17] claimed that the increase in initial lead concentration increased the ratio of the number of lead ions present in solution to the number of available adsorption sites, thus decreasing the adsorption efficiency. Nevertheless, the amount of lead adsorbed was found to increase for higher initial concentration, as shown in Run 3 and Run 16 in this study (1 and 4.5 mg lead adsorbed, respectively) due to higher collision rate between lead and soil surface.

3.5. Adsorption capacity and kinetics

Fig. 5 shows the changes in lead concentration in (a) solution and (b) soil with time at different pH values. It was found that adsorption process was

rapid at initial stage whereby high adsorption rate occurred once the solution was in contact with the sandy soil and equilibrium was achieved in less than one hour. Similar trend was also observed when iron oxide nanotubes based on maghemite, which was the type of iron in the soil studied, were used as an adsorbent for removing lead [33], copper, nickel and chromium [35]. Fast adsorption rate could be mainly due to external surface adsorption mechanism [35]. As the adsorption sites were available on the soil surface, the interactions between lead and the active sites took place readily. Thus, adsorption was rapid. Similarly, rapid adsorption process was also reported for iron oxide-coated sand whereby the equilibrium adsorption was reached within one [20,21,24] to three hours [23].

Kinetic study for lead adsorption on the sandy soil was conducted to determine the adsorption rate constant and initial adsorption rate of lead to the soil. Different kinetic models were fitted to the adsorption data. The slope, intercept and R^2 values of the linear model fitting are as shown in Table 5. The experimental data and the kinetic models were in agreement at pH 5, while the models failed to represent test data at pH 2 due to insignificant trend on lead adsorption. Table 5 shows that the result is best fit in pseudo-second-order kinetic model as this model shows relatively high R^2 at 0.9969; the curve fitting for this model is as shown in Fig. 6. This kinetic model was also accepted by researchers who utilised iron-coated sand [20,24] and maghemite nanotubes [32] in lead adsorption. From this model, the adsorption rate
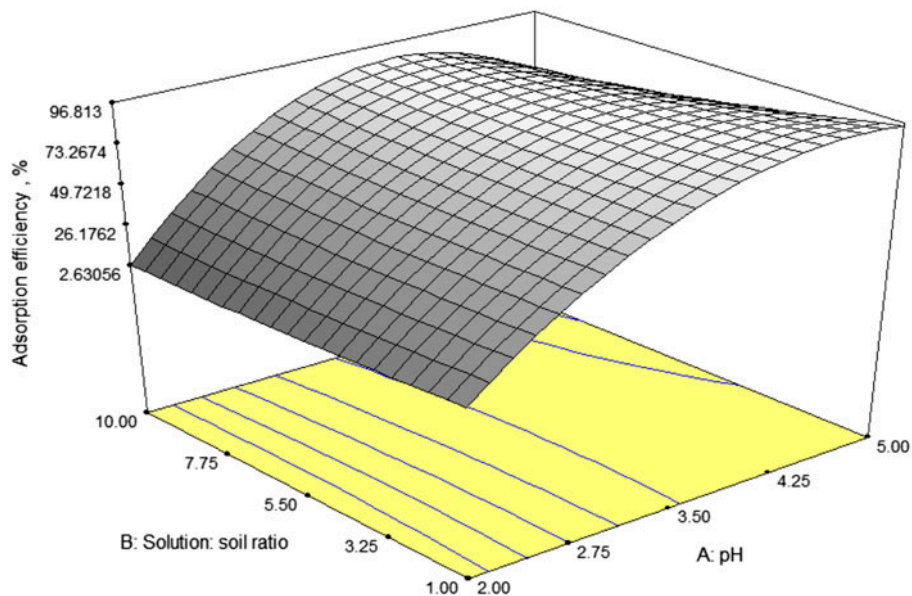

Fig. 3. Interaction effect between solution: soil ratio and pH on adsorption efficiency (initial concentration, 60 ppm).
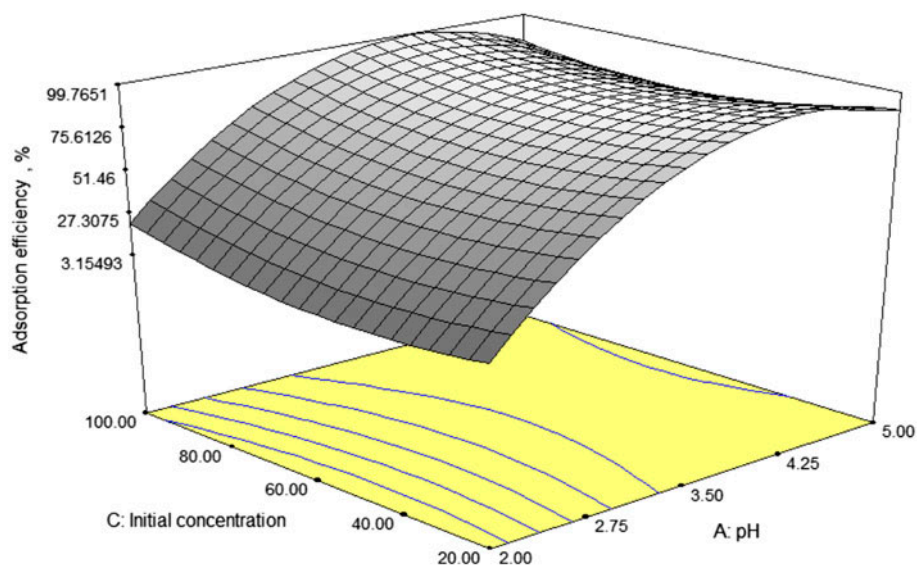
Fig. 4. Interaction effect between initial concentration and pH on adsorption efficiency (solution: soil ratio: 5.5).
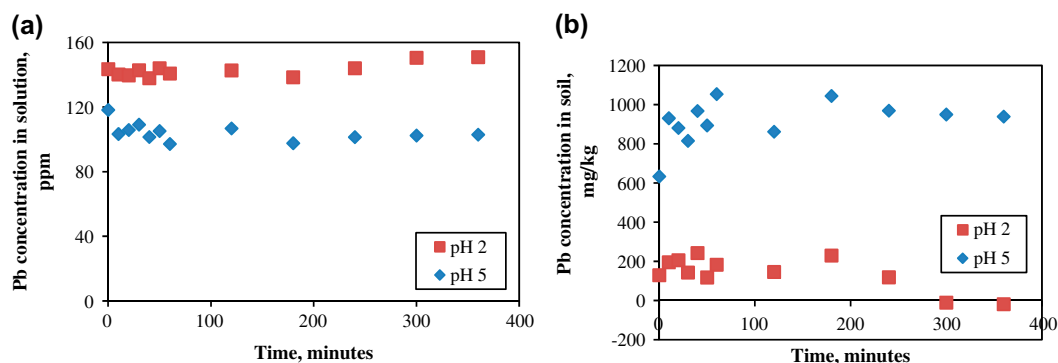

Fig. 5. Changes of lead concentration with time at different pH in: (a) solution and (b) soil.

Table 5
Slope, intercept and R^2 of the kinetic models for lead adsorption on soil under pH 5

Model	Linear equation	Slope	Intercept	R^2
Pseudo-first-order kinetic model	$\log(q_e - q_t) = \log q_e - \frac{k_{p1}}{2.303}t$	−0.003	2.0683	0.3708
Pseudo-second-order kinetic model	$\frac{t}{q_t} = \frac{1}{V_0} + \frac{1}{q_e}t; V_0 = k_{p2}q_e^2$	0.001	0.0006	0.9969
Elovich model	$q = \alpha \ln(a\alpha) + \alpha \ln t$	14.642	871.24	0.089
Second-order kinetic model	$\frac{1}{C_t} = k_2 t + \frac{1}{C_0}$	5×10^{-7}	0.0094	0.0401
Film diffusion mass transfer kinetic model	$\ln\left(1 - \frac{q_t}{q_e}\right) = -R^1 t; R^1 = \frac{3D_e^1}{r_0 \Delta r_0 k^I}$	−0.0148	0	−1.17
Double exponential model (DEM)	$\ln(q_e - q_t) = \ln\frac{D_2}{m_a} - K_2 t$	−0.0069	4.7625	0.3708

constant, initial adsorption rate and adsorption capacity for the sandy soil under investigation were determined as 0.001667/(mg/kg) min, 1,666.67 mg/kg min and 1,000 mg/kg, respectively.

3.6. Adsorption isotherm

The data points were fitted into different isotherm models in order to identify the adsorption mechanism of lead on the sandy soil. Table 6 shows that the

Table 6
Adsorption isotherms for lead adsorption on soil under pH 5

	Slope	Intercept	R^2	Q_{max}	K_L	n	K_f	A	b	β
Langmuir	0.0011	0.0047	0.9954	909.091	0.234	–	–	–	–	–
Freundlich	0.2058	2.5791	0.9876	–	–	4.859	13.185	–	–	–
Temkin	129.8	333.11	0.9945	–	–	–	–	1.476	19.088	–
DR	7.00E−07	6.6726	0.8887	790.4481	–	–	–	–	–	7.00E−07

Table 7
Comparison on the adsorption capacity of the studied soil and other modified sands

Name of adsorbent	Adsorption capacity (mg/g)	Iron content	Reference
Iron oxide-coated sand	0.3375	30 mg/g	[20]
Iron oxide-coated sand	1.211	Not mentioned	[23]
Iron oxide nanoparticle-coated sand	2.09	5.7 mg/g	[38]
Naturally iron oxide-coated sand	2.85	5.12 mg/g	[21]
Naturally iron-rich sandy soil	0.91–1.00	3.719 mg/g	Present study

results for curve fitting using Langmuir, Freundlich, Temkin and DR models. Langmuir isotherm has the best fit with R^2 value of 0.9954, and the maximum adsorption capacity is found to be 909.091 mg/kg. Several studies also reported that the adsorption of lead on iron oxide-coated sand and maghemite nanotubes followed Langmuir adsorption isotherm [21,23,24,32]. Dada et al. [36] suggested that Langmuir isotherm was valid only for monolayer adsorption on a surface containing finite number of identical sites and no transmigration of adsorbate in the plane of the surface. Thus, it could be interpreted that lead adsorption on natural high-iron content sandy soil conforms to another published works that proposed monolayer chemisorption mechanism of lead on the iron-coated sand [24] and maghemite nanotubes [32]. Chemisorption is a chemical adsorption process which occurs by the formation of chemical bond between the adsorbate

(heavy metals) and adsorbent surface (soil surface). Due to its dependency on the adsorbent surface area/ active sites, this process appears to follow a monolayer mechanism [37]. In this study, significant amount of iron (3,719 mg/kg) served as binding sites for lead adsorption on the soil and no further binding was detected after saturation, indicating the behaviour of monolayer chemisorption process.

3.7. Comparison of adsorption performance

Table 7 shows the comparative performance of different types of sands on lead adsorption. It is found that the sandy soil used in this study has comparable adsorption capacity as artificial iron oxide-coated sand [20,23,38]. The adsorption capacity is proportional to iron concentration in the soil whereby higher iron concentration provides higher adsorption capacity. This is observed in Table 7 that an iron content of >5 mg/g provides Pb adsorption capacity of >2 mg/g, whereas the present study which has 3.719 mg/g of iron content only shows 0.91–1 mg/g of adsorption capacity. However, it is worth noting that iron content is not the only factor that affects the adsorption capacity of soil as other properties such as carbonate and organic matter contents may contribute to adsorption process as well [39].

Fig. 6. Curve fitting for Pb adsorption on the sandy soil using pseudo-second-order kinetic model.

4. Conclusions

Technical feasibility of natural iron-rich sandy soil as low-cost adsorbent was investigated in this study using RSM based on Box–Behnken design. The sandy soil showed promising results for lead removal from
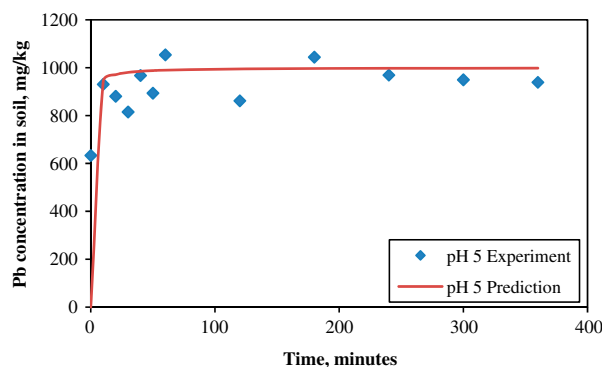
water due to its high adsorption efficiency (97%). The study revealed that pH had highest impact on the adsorption process, and in particular, pH 3.5–5 provided the best adsorption efficiency. In comparison with pH, solution: soil ratio and initial lead concentration showed minor effects. Nevertheless, lead adsorption efficiency was found to reduce significantly when solution: soil ratio was increased, especially under higher pH due to lower specific contact area for effective collision between soil and lead in the solution.

The adsorption of lead on the sandy soil was a monolayer chemisorptions process. Adsorption occurred mainly by the formation of chemical bond with the iron available on the soil. This was supported by adsorption isotherm analysis as Langmuir isotherm showed the best fit in this study. The adsorption process was rapid and was comparable to maghemite nanotubes and other iron-coated sands, as discussed in Section 3.5. The adsorption process followed pseudo-second-order kinetic model with adsorption rate constant, initial adsorption rate and adsorption capacity of 0.001667/(mg/kg) min, 1,666.67 mg/kg min and 1,000 mg/kg, respectively.

Unlike normal sand, natural iron-rich sandy soil is suitable for application as adsorbent without any surface treatment as it provides adsorption sites for lead adsorption from water with reasonable adsorption capacity (0.9–1.0 mg/g). Although it has a lower adsorption capacity in comparison with other modified sands and adsorbents, it does not need any surface modification through chemical treatment and its abundance in Hulu Langat area may offer an opportunity for its commercial use as an adsorbent for lead.

Acknowledgements

Abbreviations

A — initial adsorption rate for Elovich kinetic model (mg/(kg min))
A — Temkin isotherm equilibrium binding constant (L/kg)
A — desorption constant
B — Temkin isotherm constant
B — Dubinin–Radushkevich isotherm constant (mol^2 k/J^2)
C_0 — initial lead concentration in the solution (ppm)
C_t — lead concentration in the solution at time t (ppm)

D_e^1 — effective liquid film diffusion coefficient (cm^2/min)
D_2 — sorption rate parameters for slow step in DEM model (mg/L)
k' — equilibrium constant of adsorption for film diffusion mass transfer rate equation
k_{p1} — adsorption rate constant for pseudo-first-order kinetic model (1/min)
k_{p2} — adsorption rate constant for pseudo-second-order kinetic model (kg/(mg min))
k_2 — rate constant for second-order kinetic model (L/(mg min))
K_2 — rate constant for slow rate in DEM model (1/min)
K_f — Freundlich isotherm constant (mg/kg)
K_L — Langmuir isotherm constant (L/mg)
m_a — amount of adsorbent in the solution for DEM model (g/L)
n — adsorption intensity of the adsorbent for Freundlich isotherm
q_e — adsorption of lead per unit adsorbent at equilibrium, adsorption capacity (mg/kg)
q_t — adsorption of lead per unit adsorbent at time t (mg/kg)
Q_{max} — maximum adsorption capacity (mg/kg)
r_0 — radius of adsorbent beads (cm)
Δr_0 — thickness of liquid film (cm)
R^1 — liquid film diffusion constant (1/min)
T — time (min)
V_0 — initial sorption rate for pseudo-second-order kinetic model (mg/(kg min))

References

[1] Department-of-Environment-Malaysia, Environmental Quality (Industrial Effluent) Regulation 2009, in http://www.doe.gov.my/files/multimedia141/EFLUEN___PERINDUSTRIAN___2009_1.pdf, 2009.

[2] J.O. Duruibe, M.O.C. Ogwuegbu, J.N. Egwurugwu, Heavy metal pollution and human biotoxic effects, Int. J. Phys. Sci. 2(5) (2007) 112–118.

[3] R.A. Wuana, F.E. Okieimen, Heavy metals in contaminated soils: A review of sources, chemistry, risks and best available strategies for remediation, Int. Scholarly Res. Network Ecol. 2011 (2011) 1–20.

[4] M.N. Rashed, Adsorption technique for the removal of organic pollutants from water and wastewater, in: M.N. Rashed (Ed.), Organic Pollutants–Monitoring, Risk and Treatment, InTech, Rijeka, 2013, pp. 167–194.

[5] M. Grassi, G. Kaykioglu, V. Belgiorno, G. Lofrano, Removal of emerging contaminants from water and wastewater by adsorption process, in: G. Lofrano (Ed.), Emerging Compounds Removal from Wastewater, Springer, Dordrecht, 2012, pp. 15–37.

[6] Ö. Gerçel, H.F. Gerçel, Adsorption of lead(II) ions from aqueous solutions by activated carbon prepared from biomass plant material of *Euphorbia rigida*, Chem. Eng. J. 132(1–3) (2007) 289–297.

[7] M. Momčilović, M. Purenović, A. Bojić, A. Zarubica, M. Ranđelović, Removal of lead(II) ions from aqueous solutions by adsorption onto pine cone activated carbon, Desalination 276(1–3) (2011) 53–59.

[8] K. Zhang, W.H. Cheung, M. Valix, Roles of physical and chemical properties of activated carbon in the adsorption of lead ions, Chemosphere 60(8) (2005) 1129–1140.

[9] M. Imamoglu, O. Tekir, Removal of copper (II) and lead (II) ions from aqueous solutions by adsorption on activated carbon from a new precursor hazelnut husks, Desalination 228 (2008) 108–113.

[10] M. Machida, B. Fotoohi, Y. Amamo, L. Mercier, Cadmium(II) and lead(II) adsorption onto hetero-atom functional mesoporous silica and activated carbon, Appl. Surf. Sci. 258(19) (2012) 7389–7394.

[11] L. Dong, Z. Zhu, H. Ma, Y. Qiu, J. Zhao, Simultaneous adsorption of lead and cadmium on MnO_2-loaded resin, J. Environ. Sci. 22(2) (2010) 225–229.

[12] A. Örnek, M. Özacar, İ.A. Şengil, Adsorption of lead onto formaldehyde or sulphuric acid treated acorn waste: Equilibrium and kinetic studies, Biochem. Eng. J. 37(2) (2007) 192–200.

[13] S. Bhattacharjee, S. Chakrabarty, S. Maity, S. Kar, P. Thakur, G. Bhattacharyya, Removal of lead from contaminated water bodies using sea nodule as an adsorbent, Water Res. 37(16) (2003) 3954–3966.

[14] L.-M. Zhang, D.-Q. Chen, An investigation of adsorption of lead(II) and copper(II) ions by water-insoluble starch graft copolymers, Colloid. Surf. A. 205(3) (2002) 231–236.

[15] E.S.Z. El-Ashtoukhy, N.K. Amin, O. Abdelwahab, Removal of lead (II) and copper (II) from aqueous solution using pomegranate peel as a new adsorbent, Desalination 223(1–3) (2008) 162–173.

[16] S.A. Al-Jlil, F.D. Alsewailem, Saudi Arabian clays for lead removal in wastewater, Appl. Clay Sci. 42(3–4) (2009) 671–674.

[17] I. Chaari, E. Fakhfakh, S. Chakroun, J. Bouzid, N. Boujelben, M. Feki, F. Rocha, F. Jamoussi, Lead removal from aqueous solutions by a Tunisian smectitic clay, J. Hazard. Mater. 156(1–3) (2008) 545–551.

[18] H. Chen, A. Wang, Kinetic and isothermal studies of lead ion adsorption onto palygorskite clay, J. Colloid Interface Sci. 307(2) (2007) 309–316.

[19] M. Şölener, S. Tunali, A.S. Özcan, A. Özcan, T. Gedikbey, Adsorption characteristics of lead(II) ions onto the clay/poly(methoxyethyl)acrylamide (PMEA) composite from aqueous solutions, Desalination 223 (1–3) (2008) 308–322.

[20] N.S. Ahmedzeki, Adsorption filtration technology using iron-coated sand for the removal of lead and cadmium ions from aquatic solutions, Desalin. Water Treat. 51(28–30) (2013) 1–7.

[21] N. Boujelben, J. Bouzid, Z. Elouear, Studies of lead retention from aqueous solutions using iron-oxide-coated sorbents, Environ. Technol. 30(7) (2009) 737–746.

[22] C. Lai, C. Gao, T. Lin, S. Yeh, C. Chen, M. Wang, Simulation of lead ions adsorption onto the iron-coated medium: Dependent on temperature and pH, Pract. Period. Hazard. Toxic Radioact. Waste Manage. 10(1) (2006) 28–32.

[23] C.H. Lai, C.Y. Chen, Removal of metal ions and humic acid from water by iron-coated filter media, Chemosphere 44(5) (2001) 1177–1184.

[24] M. Mohapatra, S. Khatun, S. Anand, Adsorption behaviour of Pb(II), Cd(II) and Zn(II) on NALCO plant sand, Indian J. Chem. Technol. 16(4) (2009) 291–300.

[25] C.D. Montgomery, Design and Analysis of Experiments, fifth ed., Wiley, New York, NY, 2001.

[26] B. Shokri, M.A. Firouzjah, S.I. Hosseini, FTIR analysis of silicon dioxide thin film deposited by metal organic-based PECVD, in: 19th International Symposium on Plasma Chemistry, Bochum, 2009.

[27] A.M. Avram, A. Radoi, V. Schiopu, M. Avram, H. Gavrila, Synthesis and characterization of γ-Fe2O3 nanoparticles for applications in magnetic hyperthermia, in: 2011 Soft Magnetic Materials Conference, Kos, 2011.

[28] J.C. Rubim, M.H. Sousa, J.C.O. Silva, F.A. Tourinho, Raman spectroscopy as a powerful technique in the characterization of ferrofluids, Braz. J. Phys. 31 (2001) 402–408.

[29] S.K. Sahoo, K. Agarwal, A.K. Singh, B.G. Polke, K.C. Raha, Characterization of γ- and α-Fe2O3 nano powders synthesized by emulsion precipitation–calcination route and rheological behaviour of α-Fe2O3, Int. J. Eng. Sci. Technol. 2(8) (2010) 118–126.

[30] K.S.W. Sing, D.H. Everett, R. Haul, L. Moscou, R.A. Pierotti, J. Rouquerol, T. Siemieniewska, Reporting physisorption data for gas/solid system with special reference to the determination of surface area and porosity, Pure Appl. Chem. 54(11) (1982) 2201–2218.

[31] S.-J. Park, M.-K. Seo, Interface Science and Composites. Academic Press, Boston, MA, 2011.

[32] A. Roy, J. Bhattacharya, Removal of Cu(II), Zn(II) and Pb(II) from water using microwave-assisted synthesized maghemite nanotubes, Chem. Eng. J. 211–212 (2012) 493–500.

[33] Z. Cheng, A.L.K. Tan, Y. Tao, D. Shan, K.E. Ting, X.J. Yin, Synthesis and characterization of iron oxide nanoparticles and applications in the removal of heavy metals from industrial wastewater, Int. J. Photoenergy 2012 (2012) 1–5.

[34] P. Ghaisari, S.N. Hosseini, S. Sharifnia, M. Khatami, Parameters optimization of recombinant hepatitis B antigen adsorption–desorption in purification process on three different kinds of diatomaceous earth matrix, Chem. Eng. Res. Des. 92 (2014) 2782–2791.

[35] J. Hu, G. Chen, I.M.C. Lo, M.ASCE, selective removal of heavy metals from industrial wastewater using maghemite nanoparticle: Performance and mechanisms, J. Environ. Eng. 132(7) (2006) 709–715.

[36] A.O. Dada, A.P. Olalekan, A.M. Olatunya, O. Dada, Langmuir, Freundlich, Temkin and Dubinin-Radushkevich Isotherms studies of equilibrium sorption of Zn2+ unto phosphoric acid modified rice husk, IOSR, J. Appl. Chem. 3(1) (2012) 38–45.

[37] M.A. Al-Anber, Thermodynamics approach in the adsorption of heavy metals, in: J.C. Moreno-Piraján (Ed.), Thermodynamics—Interaction Studies—Solids, Liquids and Gases. InTech, Rijeka, 2011, pp. 737–764.

[38] S.-M. Lee, C. Laldawngliana, D. Tiwari, Iron oxide nano-particles-immobilized-sand material in the treatment of Cu(II), Cd(II) and Pb(II) contaminated waste waters, Chem. Eng. J. 195–196 (2012) 103–111.

[39] L. Ma, R. Xu, J. Jiang, Adsorption and desorption of Cu(II) and Pb(II) in paddy soils cultivated for various years in the subtropical China, J. Environ. Sci. 22(5) (2010) 689–695.